Parameterized MPC to Reduce Dispersion of Road Traffic Emissions

S. K. Zegeye, B. De Schutter, J. Hellendoorn, E. A. Breunesse

Abstract— This paper has two main contributions. First, it presents a simple area-wide emission (or dispersion) model for a freeway traffic networks. The model takes the variation of the wind speed and direction into account. Second, it presents a nonlinear parameterized MPC controller for freeway traffic systems. Next, the proposed model and control approach are illustrated with a simulation-based case study. The simulation results show improved traffic performance with respect to the uncontrolled system.

I. INTRODUCTION

Frequent and sustained traffic jams are day-to-day phenomena many drivers encounter. Traffic jam related health problems and economic losses are impacting most developed countries. Despite the development of complex infrastructures and the accumulation of new knowledge and theory of traffic system, problems related to traffic jams are still escalating from time to time. Now, the introduction of intelligent transportation systems (ITS) is considered to be one of the most promising solutions in reducing the effects of traffic jams.

Another issue related to traffic systems is their impact on the environment. Due to the increase in fuel consumption and in the frequency and duration of traffic congestion as a consequence of increasing numbers of vehicles in the fleet, the emissions of road traffic systems have increased enormously. For example in most European cities road traffic emissions account for 40% volatile organic compounds, more than 70% of NO_x, and over 90% of CO [15]. Moreover, the relationship between dispersion and emissions of the traffic flow is complicated. Reduction of emissions may not reduce dispersion of emissions on specific areas near the traffic road. For example, the emission levels in areas located near freeways could be affected by the direction and the speed of the local wind.

Therefore, in order to improve the traffic flow while still guaranteeing reduced area-wide emissions, one would need to use an ITS system that controls the traffic flow in such a way that desired objectives are attained. One such solution could be the use of a control approach that adapts to the variation of the traffic system and that handles the various physical and operational constraints. In this regard, model predictive control (MPC) and other optimal control methods have been proposed in the literature [3], [8], [10]. Many

researchers have shown the potential of MPC control strategies in improving the traffic systems performance. However, despite its success in simulation-based research [3], [8], [17], the MPC control approach did not appeal to practitioners due to several reasons, the most important one of which is the intensive computation time.

In this paper, we present a special class of MPC controllers that results in lower computation times. We use parameterized MPC traffic controllers that are based on the parameterization of the traffic control measures. We further provide an area-wide emission (dispersion) model that takes the variation of the wind speed and wind direction into account. We define a multi-objective cost function based on a weighted-sum approach. The control approach and the dispersion model are illustrated with a case study.

In the next section we discuss the traffic flow and emission models considered in this paper. In Section III we present a simple area-wide dispersion model, which can be used for on-line prediction or estimation of the dispersion levels. Section IV presents the proposed control approach. In Section V we illustrate the proposed control approach and the dispersion model on a case study. Finally, we conclude the paper in Section VI.

II. TRAFFIC FLOW AND EMISSION MODELING

Since the proposed control approach requires models to predict the states and to design the control measures of the traffic system, in this section we discuss the flow and emission models employed for these purposes.

A. METANET flow model

In order to make fast on-line optimizations, we use a macroscopic traffic flow model. In particular, we select the well known macroscopic traffic flow model called METANET [12]. METANET is a second-order traffic flow model. The model describes the evolution of the traffic variables, viz. the density, the flow, and the space-mean speed, as a system of nonlinear difference equations. The METANET model is discrete both in time and space. Let T be the simulation step size and k be the simulation step counter. In the METANET model, a node is placed at a point where there is a change in the geometry of a freeway (such as a lane drop, an on/off-ramp, or a bifurcation). A homogeneous freeway that connects such nodes is called a link. Links are further divided into segments of length 500-1000 m [12]. The equations that describe the traffic dynamics

S. K. Zegeye, B. De Schutter, and J. Hellendoorn are with the Delft Center for Systems and Control, Delft University of Technology, Delft, The Netherlands. E. A. Breunesse is with Shell Nederland B.V. The Hague, The Netherlands. {s.k.zegeye, b.deschutter, j.hellendoorn}@tudelft.nl, ewald.breunesse@shell.com

in segment i of link m are given by [12], [8]

$$q_{m,i}(k) = \lambda_m \rho_{m,i}(k) v_{m,i}(k) \tag{1}$$

$$\rho_{m,i}(k+1) = \rho_{m,i}(k) + \frac{T}{L_m \lambda_m} [q_{m,i-1}(k) - q_{m,i}(k)] \tag{2}$$

$$v_{m,i}(k+1) = v_{m,i}(k) + \frac{T}{\tau} [V[\rho_{m,i}(k)] - v_{m,i}(k)]$$
$$+ \frac{T v_{m,i}(k) [v_{m,i-1}(k) - v_{m,i}(k)]}{L_m}$$
$$- \frac{T \eta [\rho_{m,i+1}(k) - \rho_{m,i}(k)]}{\tau L_m (\rho_{m,i}(k) + \kappa)} \tag{3}$$

$$V[\rho_{m,i}(k)] = \min \left\{ (\alpha_m + 1) u_{m,i}(k), \right.$$
$$\left. v_{\text{free},m} \exp\left[-\frac{1}{a_m} \left(\frac{\rho_{m,i}(k)}{\rho_{\text{cr},m}} \right)^{a_m} \right] \right\} \tag{4}$$

where $q_{m,i}(k)$, $\rho_{m,i}(k)$, and $v_{m,i}(k)$, and denote respectively the flow, density, and space-mean speed of segment i of link m at the simulation step k, $u_{m,i}(k)$ denotes the variable speed limit of segment i of link m at the simulation step k and it equal to the freeflow speed $v_{\text{free},m}$ if there is no control, L_m denotes the length of the segments of link m, and λ_m denotes the number of lanes of link m. Furthermore, $\rho_{\text{cr},m}$ is the critical density, τ a time constant, η the anticipation constant, a_m the parameter of the fundamental diagram, α_m the drivers' compliance factor, and κ is a model parameter.

For origins (such as on-ramps and mainstream entry points) a queue model is used. The dynamics of the queue length w_o at origin o are modeled as

$$w_o(k+1) = w_o(k) + T(d_o(k) - q_o(k)) \tag{5}$$

where d_o and q_o denote respectively the demand and outflow of the origin o. The outflow q_o is given by

$$q_o(k) = \min \left[d_o(k) + \frac{w_o(k)}{T}, r_o(k) C_o, \right.$$
$$\left. C_o \left(\frac{\rho_{\text{jam},m} - \rho_{m,1}(k)}{\rho_{\text{jam},m} - \rho_{\text{cr},m}} \right) \right], \tag{6}$$

with $r_o(k)$ the ramp metering rate (where $r_o \in [0\ 1]$ for a metered on-ramp and $r_o(k) = 1$ for an unmetered on-ramp or mainstream origin), $\rho_{\text{jam},m}$ the maximum density of link m, and C_o the capacity of the origin o.

B. VT-macro emission model

Since the outputs of traffic flow models are the inputs of emission models, the choice of traffic flow models dictates on the type of emission and fuel consumption that has to be used. So, we chose VT-macro [17] as emission model.

The VT-macro model is a macroscopic emission and fuel consumption model that we have in particular developed for the METANET traffic flow model. The model takes the dynamics of the average space-mean speed of the traffic flow model into account (i.e. acceleration effects are included).

Mathematically, the VT-macro model can be described as

$$J_{y,m,i}(k) = f_{y,m,i}(v_{m,i}(k), v_{m,i}(k+1), v_{m,i+1}(k+1), \rho_{m,i}(k)) \tag{7}$$

where $J_{y,m,i}(k)$[kg/s] is the estimate or prediction of the emission variable $y \in \mathscr{Y} = \{CO, NO_x, HC, CO_2\}$ of segment i of link m during the time period $[kT, (k+1)T]$ and f is a nonlinear mapping (for detailed discussion we refer to [17]).

III. DISPERSION MODELING

We define $V_{\text{w}}(k)$ as the wind speed in the time interval $[kT, (k+1)T]$ and $\varphi(k)$ as the direction of the wind in the same time interval. Here we model the dispersion of traffic emissions to a neighborhood (or target zone) near to a traffic freeway. The emissions will be considered to emanate from the center points of the segments of the freeway[1]. The emission particles will move due to wind and dispersion effects and we will capture the trajectory of the dispersion of the emissions by wavefronts moving orthogonal to the wind direction and dispersion cones.

Fig. 1(a) shows the propagation of emissions of vehicles from segment i of a link[2] m at time step k. The emissions propagate with a line wavefront in the direction of the wind. Since the emissions from vehicles are relatively more dense and have a higher temperature than the air particles, the emitted gases also expand sideways. The expansion of the emissions is inversely related to the wind speed [2]. We model this phenomenon with a divergence angle β that depends only on k. At time step k it represents the divergence angle that corresponds to half of the angle of the dispersion cone (see Fig. 1). Then, it is given by the expression

$$\beta(k) = \frac{\beta_{\max}}{1 + \beta_0 V_{\text{w}}(k)} \tag{8}$$

where $\beta_{\max} \in [0, \pi]$ is the maximum angle at which the emission is dispersed and β_0 is a model parameter.

Here we approximate wavefronts emanating from segment i by lines with $p_{l,i}$ left and bottom-most point and $p_{r,i}$ right and top-most point. Each point of the line between $p_{l,i}(k)$ and $p_{r,i}(k)$ results in a small cone due to wind and dispersion and we determine the $p_{l,i}(k+1)$ as the left and bottom-most point of all cones and the $p_{r,i}(k+1)$ as the right and top-most point of all cones. Any emissions at a point of the wavefront formed by a line segment joining the points $p_{l,i}(k)$ and $p_{r,i}(k)$ diverge with an angle equal to $\beta(k)$ both to the left and to the right of the wind direction (e.g. see the points $p_{l,i}(k)$ and $p_{r,i}(k)$ in Fig. 1(b)).

Now let us assume that a so called puff of emitted gases from segment i of the freeway in Fig. 1(a) has arrived at the wavefront formed by the line segment joining the points $p_{l,i}(k-1)$ and $p_{r,i}(k-1)$ at time step $k-1$. The emissions will further move to the next wavefront formed by the line segment joining the points $p_{l,i}(k)$ and $p_{r,i}(k)$ at wind speed $V_{\text{w}}(k-1)$ during the time period $[(k-1)T, kT]$. In general let us assume that the wind speed or direction has changed (see $V_{\text{w}}(k)$ and $\varphi(k)$ in Fig. 1(b)) at time step k. This means

---

[1]This point modeling approach can also be extended to a line modeling approach, where the emissions are considered to emanate from a center line parallel and equal to the segments.

[2]For brevity, the link index m is not used in the derivations presented in this section.

(a) Dispersion at time instant kT
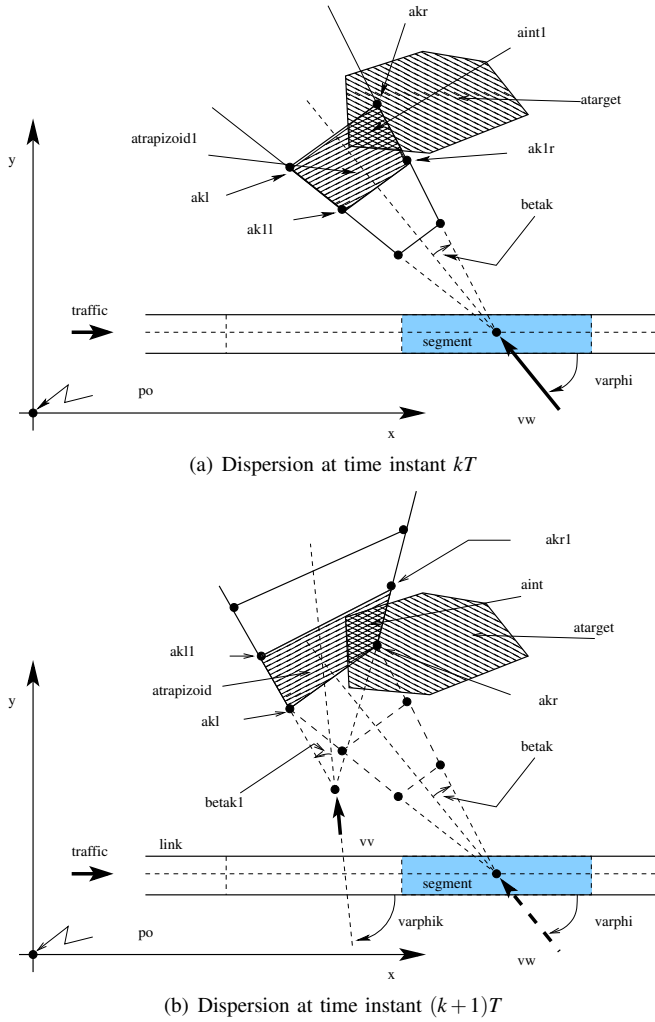

(b) Dispersion at time instant $(k+1)T$

Fig. 1. Schematic representation of horizontal dispersion of vehicle emissions with varying wind speed and angle.

that the dispersion speed and direction at every point of the wavefront will change. Then, the evolution of the end points of the wavefronts $p_{l,i}(k+1) = (x_{l,i}(k+1), y_{l,i}(k+1))$ and $p_{r,i}(k+1) = (x_{r,i}(k+1), y_{r,i}(k+1))$ is then respectively modeled as

$$x_{l,i}(k+1) = x_{l,i}(k) - TV_w(k)\frac{\cos(\varphi(k) - \beta(k))}{\cos(\beta(k))},$$

$$y_{l,i}(k+1) = y_{l,i}(k) + TV_w(k)\frac{\sin(\varphi(k) - \beta(k))}{\cos(\beta(k))},$$

$$x_{r,i}(k+1) = x_{r,i}(k) - TV_w(k)\frac{\cos(\varphi(k) + \beta(k))}{\cos(\beta(k))},$$

$$y_{r,i}(k+1) = y_{r,i}(k) + TV_w(k)\frac{\sin(\varphi(k) + \beta(k))}{\cos(\beta(k))}$$

for $\cos(\beta(k)) \neq 0$.

Consider the wavefront formed by $p_{l,i}(k)$ and $p_{r,i}(k)$ and let $E_{y,i}(p_{l,i}(k), p_{r,i}(k))$ be the corresponding emission level for emission $y \in \mathscr{Y}$. Then, the emission level for the next wavefront is

$$E_{y,i}(p_{l,i}(k+1), p_{r,i}(k+1)) = \gamma E_{y,i}(p_{l,i}(k), p_{r,i}(k)) \quad (9)$$

where $0 < \gamma \leq 1$ is a factor that characterizes the vertical dispersion.

Then the area that is subject to the emission $E_{y,i}(p_{l,i}(k+1), p_{r,i}(k+1))$ during the time period $[kT, (k+1)T]$ is the tetragon formed by the points $p_{l,i}(k)$, $p_{l,i}(k+1)$, $p_{r,i}(k+1)$, and $p_{r,i}(k)$. The area of this tetragon is denoted as $A_i(p_{l,i}(k), p_{l,i}(k+1), p_{r,i}(k+1), p_{r,i}(k))$. The areal-density of the emission in the time period is then given by

$$E_{\mathrm{ad},y,i}(k+1) = \frac{E_{y,i}(p_{l,i}(k+1), p_{r,i}(k+1))}{A_i(p_{l,i}(k), p_{l,i}(k+1), p_{r,i}(k+1), p_{r,i}(k))}. \quad (10)$$

Let the area of the target zone be denoted by A_{t}. The area of the intersection of the target zone and the tetragon formed by the emission wavefronts is denoted as $A_{\mathrm{int},i}(k)$. We can then compute the amount of emissions dispersed to the target area from segment i of the link as

$$E_{\mathrm{t},y,i}(k+1) = A_{\mathrm{int},i}(k)E_{\mathrm{ad},y,i}(k+1). \quad (11)$$

As wavefronts are emanating from segment i at each time step, we have to consider the sum of $E_{\mathrm{t},y,i}(k+1)$ over all wavefronts emitted in the past that intersect with the target zone. Let this total emission level be denoted by $E_{\mathrm{total},y,i}(k+1)$. Thus the emission density at the target zone over the time period $[kT, (k+1)T]$ due to link m will be

$$J_{\mathrm{D},y,m}(k) = \frac{1}{A_{\mathrm{t}}} \sum_{i \in \mathscr{S}_m} E_{\mathrm{total},y,i}(k) \quad (12)$$

where $\mathscr{S}_m$ is the set of all segments in link m.

The total emission density at the target zone over the time period $[kT, (k+1)T]$ is then the sum of all the emission densities of all the links over the time period $[kT, (k+1)T]$, and it is described as

$$J_{\mathrm{D,t},y}(k) = \sum_{m \in \mathscr{L}} J_{\mathrm{D},y,m}(k) \quad (13)$$

where $\mathscr{L}$ is the set of all links in the traffic network.

In the following section we presented the control approach we propose to reduce the emission levels in the target area.

IV. PARAMETERIZED MPC

The idea of model predictive control (MPC) [14] is based on two concepts: prediction and moving horizon. The MPC controller uses the current state of a system as initial condition and the model of the system to predict the evolution of the system state with respect to the variation of the control measures. Based on the predicted states of the system, the controller determines the value a given cost function. The controller then optimizes the sequence of control inputs in such a way that the cost function is minimized over the predicted horizon. However, only the first control input of the optimal sequence is applied to the system until the next control time step, after which the controller repeats the above process all over again using a moving horizon principle.

The main advantage of MPC is its capability to handle nonlinear models, constraints, and multi-objective cost functions. In the traffic control research world, MPC has

proven to improve the road network performance [3], [8], [18]. However, as a consequence of its high computation demands, the MPC controller is not yet implemented in practice. In this regard many papers (e.g. [7], [9], [11], [16]) dealt with the reduction of the computation time of MPC. But, none has done in a sufficiently satisfactory way to appeal to practitioners traffic systems.

One way to reduce the computation time of the MPC controller is to parametrize the control inputs with a set of few parameters [4], [9], [11], [16]. At every control time step[3] k_c, the MPC controller then optimizes the parameters of the control policy instead of the control inputs. Accordingly, in the sequel we present two traffic control measures and provide their parameterization with nonlinear state feedback control policies. Note that the parameterization is just an illustration of the control approach, but the control approach is generic.

A. Control measures

We illustrate our approach using variable speed limits and ramp metering as traffic control measures. In conventional MPC, these two control measure would have been optimized directly. Now, in the parameterized MPC controller the two control measures are determined according to control laws. The control policies (laws) of the variable speed limit and on-ramp metering can be defined in different ways. Here we just give only examples to illustrate our approach.

The control policy of the variable speed limit is defined using two nonlinear functions. One function describes the relative speed difference of a segment with respect to the speed of a downstream segment. The second is defined as the relative density difference of a segment with respect to the density of downstream segment. In both functions the relative difference between the current segment and the downstream segment of the freeway is used. This is because of the fact that drivers tend to adapt the speed of vehicles in the downstream. Mathematically, these functions are given by

$$f_{1,m}\big(v_{m,i}(k_c), v_{m,i+1}(k_c)\big) = \frac{v_{m,i+1}(k_c) - v_{m,i}(k_c)}{v_{m,i+1}(k_c) + \kappa_v}, \quad (14)$$

$$f_{2,m}\big(\rho_{m,i}(k_c), \rho_{m,i+1}(k_c)\big) = \frac{\rho_{m,i+1}(k_c) - \rho_{m,i}(k_c)}{\rho_{m,i+1}(k_c) + \kappa_\rho}, \quad (15)$$

where κ_v and κ_ρ are model parameters introduced to prevent division by 0.

Using these two functions, the control law that parametrizes the variable speed limit is chosen to be

$$u_{\mathrm{sl},m,i}(k_c + j + 1) = \theta_{0,m} v_{\mathrm{free},m} + \theta_{1,m} f_{1,m}(\cdot) + \theta_{2,m} f_{2,m}(\cdot) \quad (16)$$

where $j = 0, 1, \ldots, N_p - 1$ and $\theta_{\cdot,m}$ are the control law parameters.

The proposed parameterization has only 3 control parameters (one could also consider varying $\theta_{\cdot,m}$ over the prediction horizon) to be optimized in the parameterized MPC control strategy. This means that the speed limit controller can reduce the computation time if it is used with a freeway link with more than three independent variable speed limits (since there are at least $3 \times N_p$ speed limit variables over the prediction horizon in the conventional MPC).

Usually, the speed limits are constrained as $L_l \le u_{\mathrm{sl},m,i}(k_c + j + 1) \le L_u$, where L_l and L_u are respectively the lower and upper speed limits.

Using a similar reasoning as for (15), we define the parameterization of the ramp metering controller to be

$$u_{\mathrm{r},m,i}(k_c + j + 1) = u_{\mathrm{r},m,i}(k_c + j) + \theta_{3,m} \frac{\rho_{\mathrm{cr},m} - \rho_{m,i}(k_c + j)}{\rho_{\mathrm{cr},m}} \quad (17)$$

where $j = 0, 1, \ldots, N_p - 1$ and $\theta_{3,m}$ is the control law parameter.

Similar to the speed limit control, the ramp metering rate is constrainted $0 \le u_{\mathrm{r},m,i}(k_c + 1) \le 1$.

B. Performance measure

As a performance measure of the parameterized MPC controller we consider the following measure[4]:

$$J(k_c) = \zeta_1 \frac{\mathrm{TTS}(k_c)}{\mathrm{TTS_n}} + \zeta_2 \frac{\mathrm{TE}(k_c)}{\mathrm{TE_n}} + \zeta_3 \frac{\mathrm{DL}(k_c)}{\mathrm{DL_n}} + \zeta_4 \frac{\Delta(k_c)}{\Delta_n} \quad (18)$$

where $\zeta_n \ge 0$ for $n = 1, 2, 3, 4$ are weighting coefficients,

$$\mathrm{TTS}(k_c) = T \sum_{k=Mk_c}^{MN_p - 1} \left(\sum_{(m,i) \in \mathscr{I}_{\mathrm{all}}} \lambda_m L_m \rho_{m,i}(k) + \sum_{o \in \mathscr{O}_{\mathrm{all}}} w_o(k) \right),$$

$$\mathrm{TE}(k_c) = \sum_{y \in \mathscr{Y}} \mu_y \frac{\mathrm{TE}_y(k_c)}{\mathrm{TE}_{y,\mathrm{n}}}, \quad \mathrm{DL}(k_c) = \sum_{y \in \mathscr{Y}} \mu_y \frac{\mathrm{DL}_y(k_c)}{\mathrm{DL}_{y,\mathrm{n}}},$$

$$\Delta(k_c) = \sum_{k=Mk_c}^{MN_p - 1} \sum_{s \in \mathscr{S}_{\mathrm{all}}} \bigg(\|u_s(k) - u_s(k-1)\|_2^2 + \|u_s(k) - u_{s-1}(k)\|_2^2 \bigg),$$

with

$$\mathrm{TE}_y(k_c) = \sum_{k=Mk_c}^{MN_p - 1} \sum_{(m,i) \in \mathscr{I}_{\mathrm{all}}} J_{y,m,i}(k),$$

$$\mathrm{DL}_y(k_c) = \big\| [J_{\mathrm{D,t},y}(Mk_c) \ldots J_{\mathrm{D,t},y}(MN_p - 1)]^\top \big\|_\infty,$$

μ_y denoting the weights of the emissions $y \in \mathscr{Y}$, and $\mathscr{I}_{\mathrm{all}}$ and $\mathscr{O}_{\mathrm{all}}$ denoting respectively the set all segment-link pairs and the set of all origins in the traffic network and $\mathscr{S}_{\mathrm{all}}$ denoting the set of all speed limits. Moreover, the nominal values of the TTS, TE, TE_y, DL, DL_y, and Δ_n are computed by simulating the uncontrolled traffic system with all speed limits set to $v_{\mathrm{free},m}$ and all on-ramp metering set to 1.
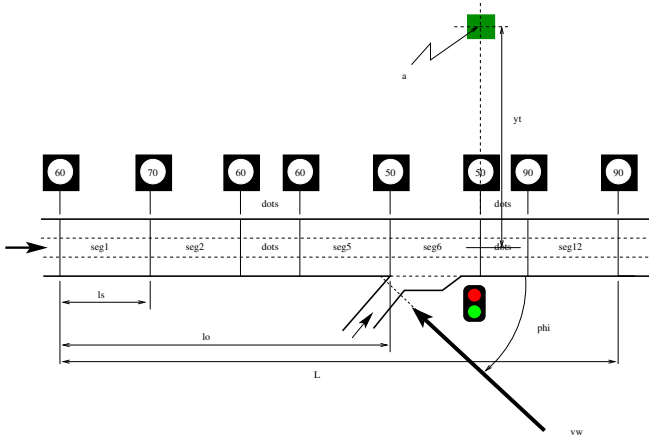
Fig. 2.   A 12 km freeway with 12 variable speed limits and one on-ramp.

Fig. 3.   Dispersion level for different control objectives.

C. Optimization method

One of the bottlenecks in MPC control approach is the extensive optimization and the resulting computational requirements. The parameterized MPC optimization problem considered for this paper is nonlinear and nonconvex. Thus a proper choice of an optimization technique has to be made in order to obtain feasible optimal control values. Owing to the nonconvex nature of the objective function, global or multi-start local optimization methods are required. Hence, multi-start sequential quadratic programming [13, Section 5.3], pattern search [1], genetic algorithms [5], or simulated annealing [6] can be used.

V. CASE STUDY

A. Freeway set up

In order to illustrate the proposed control approach and the area-wide emission modeling we consider a case study with a 12 km three-lane freeway stretch. The freeway is divided into 12 equal segments with an on-ramp at the sixth segment from the left (see Fig. 2) and each segment is provided with a variable speed limit.

The freeway is subject to wind with speed and direction given by

$$V_w(k) = 7 + 2\sin(0.005\pi k + \pi/6)\sin(0.01\pi k) \qquad (19)$$

$$\varphi(k) = \frac{2\pi}{5} + \frac{\pi}{4}\cos(0.004\pi k) \qquad (20)$$

where the wind speed $V_w(k)$ is expressed in m/s and the wind direction (angle) $\varphi(k)$ in radians. Since the dispersion is assumed unobstructed, we consider the maximum divergence of the dispersion to be $\beta_{max} = \pi$ and we set $\beta_0 = 0.6$. Moreover, the case study is simulated for over an hour.

B. Performance measures

We consider a multi-objective performance criterion that accommodates the emissions, dispersion of emissions, and travel time. The multi-objective function is defined as (18). In particular, we consider the objective function with $\mu_y = 1$ and five different combinations of ζ_n for $n = 1, 2, 3, 4$. In all these combinations $\zeta_4 = 0.01$, because we want to give
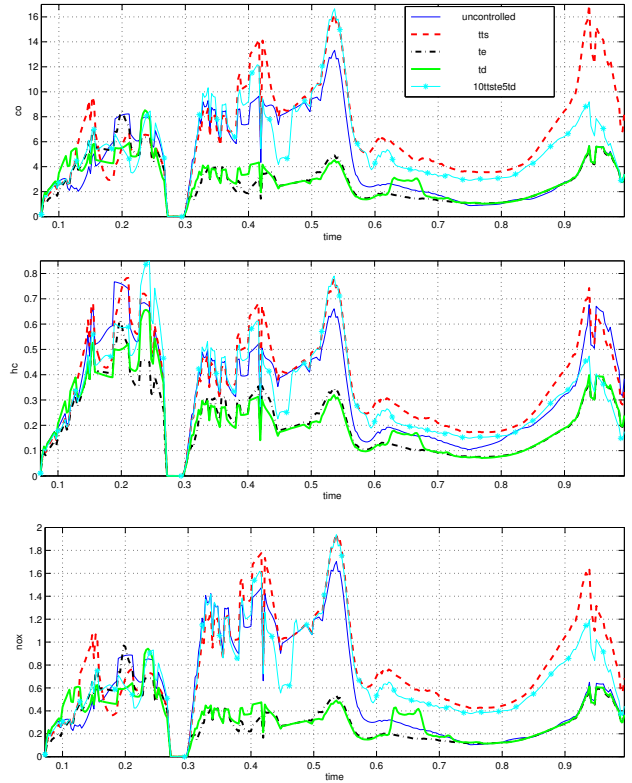
less emphasis on the variation of the control inputs. The combination of the remaining weights is tabulated in Table I along with the results of the simulations. Moreover, the nominal values of the performance criteria are determined by simulating the uncontrolled traffic system with $v_{free}m = 120$ km/h.

C. Results and discussion

We simulate the system for uncontrolled and controlled cases. In the controlled cases we consider different scenarios by varying the weightings of the objective function given in (18). The simulation results for these scenarios are tabulated in Table I. The percentail change of in either of the TTS, TE, or Total DL is described in comparison to the uncontrolled case.

The evolution of the total dispersion level in the target area is presented in Fig. 3. The figure depicts the total dispersion for different control objectives. It shows that the dispersion level becomes higher than the uncontrolled case if the control objective is to reduce total time spent (TTS) or the combination of TTS, total emissions (TE), and total dispersion level (DL) (see also Table I).

Moreover, when the objective of the controller is set to either reduce the total emissions or the dispersion level, the travel time increases by more than 10% relative to the uncontrolled case. However, both the total dispersion and the total emission are then reduced respectively by more than 33% and 47% as compared to the uncontrolled case.

TABLE I
SIMULATION RESULTS FOR DIFFERENT SCENARIOS.

Scenarios	Performance measure					
	TTS		TE		Total DL	
	[veh.h]	(g%)	[kg]	(g%)	[mg/m^{2}s]	(g%)
Uncontrolled	1362.1	(–)	127.5	(–)	1.8	(–)
TTS	875.3	(-35.7)	145.4	(+14.0)	2.6	(+44.4)
TE	1590.3	(+16.8)	66.4	(-47.9)	1.2	(-33.3)
DL	1509.0	(+10.8)	70.8	(-44.5)	1.2	(-33.3)
5TE + DL	1532.0	(+12.5)	67.7	(-46.9)	1.3	(-27.8)
10TTS+TE+5DL	874.1	(-35.8)	120.3	(-5.6)	2.3	(+27.8)

The (g%) value denotes the percentail change of the variables with respect to the uncontrolled scenario ('-' means decrement and '+' means increment).

An important point to notice here is the difference in TTS when the objective of the controller is to reduce either TE only or DL only. When the objective is the DL, the TTS becomes less worst than when the objective of the controller is to reduce TE (see Table I). This is because of the fact that when the controller is focusing on the reduction of TE, it will reduce the emissions caused by all vehicles over the whole traffic network. However, when the intention of the controller is to reduce the dispersion in the target area, it only focuses on the reduction of the emissions caused by the traffic networks that affect this particular target. Thus, the traffic networks that do not emit emissions that affect the target area could have better traffic flow.

VI. CONCLUSIONS AND FUTURE WORK

We have presented a simple area-wide emission (dispersion of emission) model that includes time-varying wind speed and wind direction. Moreover, we have presented nonlinear control policies that describe the parameterization of the traffic control measures so that nonlinear parameterized MPC can be used. We have demonstrated the proposed control approach and the model with a simulation based case study. We have considered different scenarios (both uncontrolled and controlled cases) to illustrate the potential of the parameterized MPC controller for traffic systems.

In our future work, we will extend the area-wide emission model from a point model to a full 2D model. We will compare the performance of the parameterized MPC controller with conventional MPC and consider more complicated case studies. Moreover, we will investigate the effect and correlation of queue length formed by ramp metering and the emissions dispersion.

REFERENCES

[1] C. Audet and J. E. Dennis Jr. Analysis of generalized pattern searches. *SIAM Journal on Optimization*, 13(3):889–903, 2007.

[2] C. J. Baker. Outline of a novel method for the prediction of atmospheric pollution dispersal from road vehicles. *Journal of Wind Engineering and Industrial Aerodynamics*, 65(1-3):395–404, 1996.

[3] T. Bellemans, B. De Schutter, and B. De Moor. Model predictive control for ramp metering of motorway traffic: A case study. *Control Engineering Practice*, 14(7):757–767, July 2006.

[4] A. Casavola, D. Famularo, and G. Franze. A predictive control strategy for norm-bounded LPV discrete-time systems with bounded rates of parameter change. *International Journal of Robust and Nonlinear Control*, 18(7):714–740, August 2007.

[5] L. Davis, editor. *Handbook of Genetic Algorithms*. Van Nostrand Reinhold, New York, USA, 1991.

[6] R. W. Eglese. Simulated annealing: A tool for operations research. *European Journal of Operational Research*, 46(3):271–281, 1990.

[7] P. J. Goulart, E. C. Kerrigan, and M. Maciejowski. Optimization over state feedback policies for robust control with constraints. *Automatica*, 42(4):523–533, April 2006.

[8] A. Hegyi, B. De Schutter, and H. Hellendoorn. Model predictive control for optimal coordination of ramp metering and variable speed limits. *Transportation Research Part C*, 13(3):185–209, June 2005.

[9] M. V. Kothare, V. Balakrishnan, and M. Morari. Robust constrained model predictive control using linear matrix inequalities. *Automatica*, 32(10):1361–1379, 1996.

[10] A. Kotsialos and M. Papageorgiou. Nonlinear optimal control applied to coordinated ramp metering. *IEEE Transactions on Control Systems Technology*, 12(6):920–933, November 2004.

[11] J. Löfberg. Approximations of closed loop minimax MPC. In *Proceedings of the 42nd IEEE Conference on Decision and Control*, pages 1438–1442, Maui, Hawaii, USA, December 2003.

[12] A. Messmer and M. Papageorgiou. METANET: A macroscopic simulation program for motorway networks. *Traffic Engineering and Control*, 31(9):466–470, 1990.

[13] P. M. Pardalos and M. G. C. Resende. *Handbook of Applied Optimization*. Oxford University Press, Oxford, UK, 2002.

[14] J.B. Rawlings and D.Q. Mayne. *Model Predictive Control: Theory and Design*. Nob Hill Publishing, Madison, Wisconsin, 2009.

[15] S. Schmidt and R. P. Schäfer. An integrated simulation systems for traffic induced air pollution. *Environmental Modeling & Software*, 13(3-4):295–303, 1998.

[16] R. S. Smith. Robust model predictive control of constrained linear systems. In *Proceedings of the 2004 American Control Conference*, pages 245–250, Boston, Massachusetts, USA, June 2004.

[17] S. K. Zegeye, B. De Schutter, J. Hellendoorn, and E. A. Breunesse. Model-based traffic control for balanced reduction of fuel consumption, emissions, and travel time. In *Proceedings of the 12th IFAC Symposium on Transportation Systems*, pages 149–154, Redondo Beach, California, USA, September 2009.

[18] J. Zhang, A. Boiter, and P. Ioannou. Design and evaluation of a roadway controller for freeway traffic. In *Proceedings of the 8th International IEEE Conference on Intelligent Transportation Systems*, pages 543–548, Vienna, Austria, September 2005.